

## ORIGINAL ARTICLE

# Differences in Rhythmic Neural Activity Supporting the Temporal and Spatial Cueing of Attention

Chloe E. Meehan<sup>1,2</sup>, Alex I. Wiesman<sup>3,4</sup>, Rachel K. Spooner<sup>1,4</sup>, Mikki Schantell<sup>1,4</sup>, Jacob A. Eastman<sup>1</sup> and Tony W. Wilson<sup>1,2,4</sup>

<sup>1</sup>Institute for Human Neuroscience, Boys Town National Research Hospital, Boys Town, NE 68010, USA,

<sup>2</sup>Department of Psychology, University of Nebraska, Omaha, NE 68182, USA, <sup>3</sup>Montreal Neurological Institute, McGill University, Montreal, QC H3A 2B4, Canada and <sup>4</sup>College of Medicine, University of Nebraska Medical Center, Omaha, NE 68198, USA

Address correspondence to Tony W. Wilson, Institute for Human Neuroscience, Boys Town National Research Hospital, Boys Town, NE 68010, USA. Email: [tony.wilson@boystown.org](mailto:tony.wilson@boystown.org)

## Abstract

The neural processes serving the orienting of attention toward goal-relevant stimuli are generally examined with informative cues that direct visual attention to a spatial location. However, cues predicting the temporal emergence of an object are also known to be effective in attentional orienting but are implemented less often. Differences in the neural oscillatory dynamics supporting these divergent types of attentional orienting have only rarely been examined. In this study, we utilized magnetoencephalography and an adapted Posner cueing task to investigate the spectral specificity of neural oscillations underlying these different types of attentional orienting (i.e., spatial vs. temporal). We found a spectral dissociation of attentional cueing, such that alpha (10–16 Hz) oscillations were central to spatial orienting and theta (3–6 Hz) oscillations were critical to temporal orienting. Specifically, we observed robust decreases in alpha power during spatial orienting in key attention areas (i.e., lateral occipital, posterior cingulate, and hippocampus), along with strong theta increases during temporal orienting in the primary visual cortex. These results suggest that the oscillatory dynamics supporting attentional orienting are spectrally and anatomically specific, such that spatial orienting is served by stronger alpha oscillations in attention regions, whereas temporal orienting is associated with stronger theta responses in visual sensory regions.

**Key words:** attentional orienting, magnetoencephalography, neural oscillations, spatial attention, temporal attention

## Introduction

Goal-directed attentional orienting is a process in which top-down cognitive control allows for the preferential neural processing of relevant stimuli (Posner 1980; Yantis 2002). In experimental settings, this orienting process is commonly driven by some form of cue, which signals the forthcoming appearance of a task-relevant target stimulus and grants contextual information for visual detection to optimize behavior in terms of attention and learning (Chun and Jiang 1998; Chun 2000; Atkinson et al. 2018; Jiang and Sisk 2020). Most commonly, cueing is implemented in the form of a spatial indicator that predicts

the spatial location of upcoming visual stimuli (Higuchi et al. 2016), but attentional cues may also serve as temporal indicators of the emergence of a stimulus (Olson and Chun 2001). In terms of the neural dynamics serving attentional orienting, there are a series of well-studied functional networks that are implicated in this cognitive process. Briefly, the dorsolateral prefrontal cortex (dlPFC), temporoparietal junction (TPJ), superior parietal, and higher visual areas (Clark and Hillyard 1996; Corbetta and Shulman 2002; Snyder and Chatterjee 2006; Nagata et al. 2012; Chang et al. 2013) are known to be essential cortical regions for the orienting and reorienting of attention in the human brain. However,

the cognitive neuroimaging community has also historically been biased toward the use of spatial rather than temporal cues in studying the cortical areas related to attentional orienting (Corbetta and Shulman 2002; Doesburg et al. 2016; Proskovec et al. 2018; Spooner et al. 2020b). Thus, while the networks serving spatial orienting have been studied extensively, those involved in attentional orienting in other domains have been far less examined.

Previous functional magnetic resonance imaging (MRI) work utilizing the Attention Network Test (ANT) and related attention cueing paradigms has established a neuroanatomical distinction between spatial and temporal orienting of attention. Spatial cueing of attention appears to be generally supported by the right intraparietal sulcus (IPS), left frontal eye fields, and bilateral superior parietal lobules, whereas temporal attentional cueing, or alerting, has been more frequently associated with a left hemispheric network that includes the inferior premotor cortex, IPS, and frontal regions, as well as the right TPJ (Coull and Nobre 1998; Coull et al. 2000; Fan et al. 2002; Fan et al. 2005). Though the ANT is a widely used task that probes an array of attention functions (e.g., spatial orienting, temporal orienting/alerting, and executive attention), it does have several limitations. For example, the paradigm does not balance the degree of visual stimulation across conditions, which complicates the investigation of attentional effects in many early visual regions. Additionally, in order to target each of the distinct components of attention, the ANT includes multiple conditions, but the inclusion of these multiple conditions increases the duration of the task and makes it largely infeasible for very young and older participants. The long duration also makes it difficult to implement in imaging environments where the time between successful trials needs to be extended (e.g., oscillatory analyses in magnetoencephalography or MEG; Wilson et al. 2016).

Understanding not only the spatial features of these functional brain networks, but also their temporal and spectral signatures is essential, as dynamic neural oscillations appear to represent a fundamental mechanism by which the brain organizes and transmits information. Given the well-established roles of theta (3–7 Hz) and alpha (8–13 Hz) cortical oscillations in visual attentional processing, it is likely that both of these slower-frequency oscillations participate in temporal and spatial orienting in different capacities. Theta cortical rhythms are commonly associated with the temporal segmentation of incoming visual information during the allocation of attentional resources (Jensen 2006; Busch et al. 2009; Landau and Fries 2012; Roberts et al. 2013), whereas alpha oscillations serve visuospatial attention by allowing functional disinhibition of the visual space to facilitate processing of relevant stimuli (Klimesch et al. 1998; Jensen and Mazaheri 2010; Dombrowe and Hilgetag 2014; van Diepen et al. 2016; Foster et al. 2017). Thus, given these broad associations, one might expect temporal orienting to be associated with stronger theta responses, whereas spatial orienting would be linked to more robust alpha responses. Unfortunately, this hypothesis has not yet been empirically tested.

In the current study, we recorded task-based MEG in a group of healthy young adults to probe the underlying oscillatory dynamics involved in spatial and temporal attentional orienting, to quantify the dynamics and determine whether these subprocesses are spectrally specific in the human brain. Given the limitations noted above with using the ANT in studies of oscillatory activity, we utilized a novel adaptation of the Posner (1980) cueing paradigm, which targeted differential attentional cueing effects by using 2 types of cues. Briefly, one type of cue

was temporally variable and spatially reliable, whereas the other type of cue was temporally consistent and spatially irrelevant. MEG was recorded throughout the task, enabling the precise spatiotemporal identification of the oscillatory dynamics supporting attentional cueing, which is imperative considering the rapid timescale of attentional processing (Proskovec et al. 2018; Wiesman et al. 2019; Arif et al. 2020). Given the previous literature, we hypothesized that spatial and temporal attentional orienting would involve spectrally distinct neural dynamics across attentional networks (Jensen 2006; Busch et al. 2009; Händel et al. 2011; Landau and Fries 2012; Wiesman et al. 2017b; Wiesman and Wilson 2019). More explicitly, we expected spatial orienting to elicit more robust alpha responses and temporal orienting to generate stronger theta activity in cortical areas previously associated with attentional processing.

## Materials and Methods

### Participants

Thirty-four healthy young adults between the ages of 19 and 36 (mean [M] = 26.34; standard deviation [SD] = 4.00) were recruited to participate in this study. Exclusionary criteria included any medical illness affecting central nervous system function, neurological and/or psychiatric disorder, history of head trauma, nonremovable metal implant that would adversely affect data acquisition and current substance abuse. All participants had normal or corrected-to-normal vision. Each participant provided written informed consent and was compensated for their time and travel. The Institutional Review Board at the University of Nebraska Medical Center reviewed and approved this study, and all protocols were in accordance with the Declaration of Helsinki.

### Experimental Paradigm and Behavioral Analysis

For MEG recording, participants were seated in a nonmagnetic chair within a magnetically shielded room, with their heads positioned within the sensor array. During recording, each participant completed a novel adaptation of the Posner cueing task in which all trials were validly cued (Posner 1980). Participants were instructed to maintain fixation on a centrally presented square throughout the task, which encompassed 2 diagonal lines to form an “X” (Fig. 1). Each trial began with the presentation of the fixation box for 2200 ms ( $\pm 200$  ms). Next, 2 adjacent, bisected segments of the X within the fixation square were shaded to form an arrow, which served as the cue. Shading of the 2 rightmost segments created an arrow pointing to the left, and similar right, up, and down facing arrows were created by shading the 2 leftmost, 2 lower, and 2 upper segments, respectively. For one half of all trials presented to each participant, the direction of this cue provided information regarding the spatial location of the upcoming target stimulus but no information regarding its timing. On the other half of trials, the cue provided useful information regarding when the upcoming target would appear but no information regarding its spatial location. For the trials where a spatial cue was presented, this cue would remain for a randomly jittered interval of  $900 \pm 400$  ms, whereas for temporal cues a fixed interval of 900 ms was used. Importantly, whether the left/right or up/down cue pairs provided the spatial or temporal information was counterbalanced across participants. In other words, for one-half of all participants, the left/right arrows would indicate the

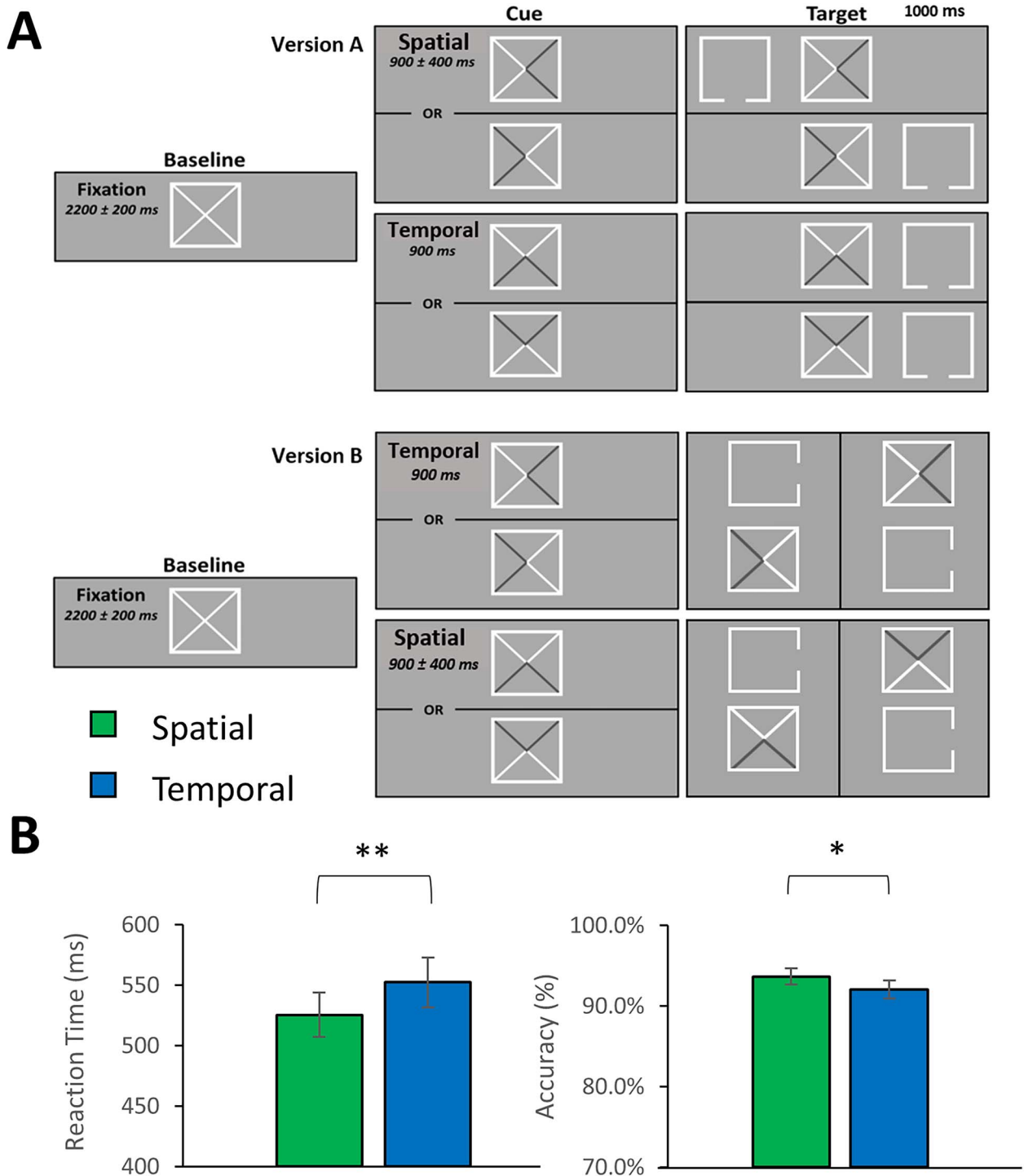


**Figure 1.** Attentional cueing task and behavioral performance. (A) A fixation box with 2 diagonal lines was presented for 2200 ( $\pm 200$ ) ms, followed by either a spatial cue (version 1: shaded arrow pointing left or right; version 2: shaded arrow pointing up or down) for 900 ( $\pm 400$ ) ms or a temporal cue (version 1: shaded arrow pointing up or down; version 2: shaded arrow pointing left or right) for 900 ms. The target stimulus then appeared to one side of the cue (version 1: left or right; version 2: top or bottom) for 1000 ms. Participants responded regarding the location of the opening on the target stimulus (version 1: top = right middle finger, bottom = right index finger; version 2: right = right index finger, left = right middle finger). Note for both conditions in version 2 of the task, the cue panel on the top corresponds with the target panel on the left and the bottom cue panel precedes the right target panel. Importantly, the version of the task administered was counterbalanced across participants. (B) Metrics for behavior are presented on the y-axis and the 2 conditions (spatial vs. temporal) are separated on the x-axis. Participants responded more quickly ( $P < 0.001$ ) and accurately ( $P = 0.034$ ) in the spatially relative to the temporally cued trials. \* $P < 0.05$ . \*\* $P < 0.001$ .

spatial location of the upcoming target, whereas for the other half the up/down arrows would provide this information. Furthermore, whether the target stimuli were presented on the right and left or the top and bottom of the central fixation box for each participant was covaried as a function of the spatial cues and held constant across both conditions for each participant. Note that the location of the target was also balanced across all trials. The target consisted of an empty box with an opening on one side, presented for 1000 ms, which was covaried to never match the direction of the spatial cues (e.g., openings were on the left/right when the spatial cues pointed up/down). Participants were instructed to indicate by button press the side of the box on which the opening appeared (right index = bottom/right; right middle finger = top/left). The 2 versions of the task are shown in Figure 1A, and the instructions given to the participants are provided in the Supplementary Methods. On average, each trial lasted 4100 ms, and each participant completed a total of 200 trials, with 100 being spatially cued and 100 temporally cued, equating to a total run time of about 14 min. Finally, note that this task was one of 4 tasks completed in the scanner during the study visit. Data from the other 3 experiments, which were unrelated to the current attentional orienting task, will be reported in later manuscripts.

### MEG Data Acquisition

MEG data acquisition, structural coregistration, preprocessing, and sensor-/source-level analyses followed a similar pipeline as a number of previous manuscripts from our laboratory (Wiesman et al. 2017a; Kurz et al. 2018; Proskovec et al. 2018; Spooner et al. 2018, 2019; Wiesman and Wilson 2019, 2020a). All recordings took place in a 1-layer magnetically shielded room with active shielding engaged for environmental noise compensation. A 306-sensor Elekta/MEGIN MEG system (Helsinki, Finland), equipped with 204 planar gradiometers and 102 magnetometers, was used to sample neuromagnetic responses continuously at 1 kHz with an acquisition bandwidth of 0.1–30 Hz. Participants were monitored by a real-time audio–video feed from inside the shielded room during MEG data acquisition. Each MEG dataset was individually corrected for head motion and subjected to noise reduction using the signal space separation method with a temporal extension (MaxFilter v2.2; correlation limit: 0.950; correlation window duration: 6 s (Taulu and Simola 2006).

### Structural MRI Processing and MEG Coregistration

Prior to MEG acquisition, 4 coils were attached to the participants' heads and localized, together with the 3 fiducial points and scalp surface, using a 3-D digitizer (Fastrak 3SF0002, Polhemus Navigator Sciences, Colchester, VT). Once positioned in the MEG, the coils produced an electrical current with a unique frequency label and an accompanying measurable magnetic field, which allowed each coil to be localized in reference to the MEG instrument sensors throughout recording. Since coil locations were also known in head coordinates, all MEG measurements could be transformed into a common coordinate system. With this coordinate system, each participant's MEG data were coregistered with their individual structural  $T_1$ -weighted MRI data using BESA MRI (version 2.0) prior to source-space analysis. Structural MRI data were aligned parallel to the anterior and posterior commissures and transformed into standardized Talairach space. Following source analysis (i.e., beamforming), each participant's  $4.0 \times 4.0 \times 4.0$  mm functional images were

also transformed into standardized space using the transform that was previously applied to the structural MRI volume and spatially resampled.

### MEG Preprocessing, Time–Frequency Transformation, and Sensor-Level Statistics

Cardiac and blink artifacts were identified in the raw MEG data and removed with signal-space projection, which was subsequently accounted for during source reconstruction (Uusitalo and Ilmoniemi 1997). The continuous magnetic time series was then bandpass filtered between 0.5 and 200 Hz, plus a 60-Hz notch filter, and divided into 1500-ms epochs, with the baseline extending from –500 to 0 ms prior to the onset of the visual cue. Epochs containing artifacts were rejected using a fixed threshold method, supplemented with visual inspection. Briefly, in MEG, the raw signal amplitude is strongly affected by the distance between the brain and the MEG sensors, as the magnetic field strength falls off sharply as the distance from the current source increases. To account for this source of variance across participants, as well as other sources of variance, we used an individually determined threshold based on the within-subject signal distribution for both amplitude and gradient to reject artifacts. Across all participants, the average amplitude threshold for rejecting artifacts was 1126.03 (SD = 325.89) fT/cm and the average gradient threshold was 421.15 (SD = 142.30) fT/(cm\*ms). Across the group, an average of 167.79 (SD = 16.06) out of 200 possible trials per participant were used for further analysis in this experiment, including an average of 84.21 (SD = 8.63) out of 100 trials per participant in the spatially cued condition and an average of 83.58 (SD = 7.78) out of 100 trials per participant in the temporally cued condition. Importantly, our comparisons between the conditions were not compromised by differences in the number of accepted trials per condition, as this metric did not significantly differ across conditions ( $P > 0.20$ ).

Complex demodulation (Papp and Ktonas 1977; Kovach and Gander 2016) was used to transform the artifact-free epochs into the time–frequency domain, and the resulting spectral power estimations were averaged per sensor to generate time–frequency plots of mean spectral density. The time–frequency analysis was performed with a frequency step of 2 Hz and a time step of 25 ms between 4 and 100 Hz to observe higher frequency activity (e.g., alpha, gamma). We also used a complementary time–frequency analysis performed with a 1 Hz/50 ms resolution from 2 to 100 Hz for better identification of lower frequency activity in the theta range. These sensor-level data were then normalized by each respective bin's baseline power for visualization purposes, calculated as the mean power during the –500 to 0 ms baseline period.

The specific time–frequency windows used for source imaging were determined by statistical analysis of the sensor-level spectrograms across both conditions and the entire array of gradiometers. Each data point in each sensor-level spectrogram was initially evaluated using a mass univariate approach based on the general linear model. To reduce the risk of false positive results while maintaining reasonable sensitivity, a 2-stage procedure was followed to control for Type 1 error. In the first stage, paired sample t-tests against baseline were conducted on each data point and the output spectrogram of t-values was thresholded at  $P < 0.05$  to define time–frequency bins containing potentially significant oscillatory deviations across all participants. In stage 2, the time–frequency bins that survived the threshold were clustered with temporally and/or spectrally

neighboring bins (per sensor) that were also above the threshold ( $P < 0.05$ ), and a cluster value was derived by summing all of the  $t$ -values of all data points in the cluster. Nonparametric permutation testing was then used to derive a distribution of cluster values, and the significance level of the observed clusters (from stage one) were tested directly using this distribution (Ernst 2004; Maris and Oostenveld 2007). For each comparison, 10,000 permutations were computed to build a distribution of cluster values. Based on these analyses, rectangular time–frequency windows within significant clusters were identified and used to guide source-level analysis.

### MEG Source Analysis

Cortical sources were imaged through an extension of the linearly constrained minimum variance vector beamformer (Van Veen et al. 1997; Gross et al. 2001; Hillebrand et al. 2005), which employs spatial filters in the frequency domain to calculate source power for the entire brain volume. The single images were derived from the cross spectral densities of all combinations of MEG gradiometers averaged over the time–frequency range of interest, and the solution of the forward problem for each location on a grid specified by input voxel space. In principle, the beamformer operator generates a spatial filter for each grid point that passes signals without attenuation from the given neural region, while suppressing activity in all other brain areas. The filter properties arise from the forward solution (lead field) for each location on a volumetric grid specified by input voxel space, and from the MEG covariance matrix. Basically, for each voxel, a set of beamformer weights is determined, which amounts to each MEG sensor being allocated a sensitivity weighting for activity in the particular voxel. This set of beamformer weights is the spatial filter unique to the given voxel and this procedure is iterated until such a filter is computed for each voxel in the brain. Activity in each voxel is then determined independently and sequentially to produce a volumetric map of electrical activity with relatively high spatial resolution. In short, this method outputs a power value for each voxel in the brain, determined by a weighted combination of sensor-level time–frequency activity. Following convention, the source power in these images was normalized per participant using a prestimulus noise period (i.e., baseline) of equal duration and bandwidth (Hillebrand et al. 2005). MEG preprocessing and imaging used the Brain Electrical Source Analysis (version 7.0) software. Note that we also conducted a follow-up beamformer analysis using the magnetometer sensors and that this analysis was identical, with the exception of the input data (i.e., artifact-free magnetometer data instead of artifact-free gradiometer data).

Normalized source power was computed for the selected time frequency bands over the entire brain volume per participant at  $4.0 \times 4.0 \times 4.0$  mm resolution. Each participant's functional images were transformed into standardized space using the transform that was previously applied to the structural images and then spatially resampled. The resulting 3D maps of brain activity were averaged across participants and conditions to qualitatively assess the anatomical basis of the significant oscillatory responses identified through the sensor-level analysis. To identify the effect of cue type on oscillatory responses, we performed a whole-brain analysis of the cueing effect (i.e., spatial vs. temporal) per each oscillatory response of interest, using paired-sample  $t$ -tests. To account for multiple comparisons, we employed a nonparametric cluster-based permutation approach

similar to that performed on the sensor-level spectrograms, with an initial cluster-forming threshold of  $P < 0.001$ , 10,000 permutations, and a final cluster size threshold of  $k > 10$  and corrected significance threshold of  $P < 0.05$ . From the remaining significant clusters, pseudo  $t$ -values per condition were extracted from the peak voxels for visualization purposes. Cluster-based permutation testing on sensor-array and source-level data was performed in BESA Statistics (v2.0).

### Virtual Sensor Extraction for Single-Trial Analyses and Intertrial Phase Coherence

Using the peak voxel locations identified in the whole-brain statistical analysis, virtual sensor data were computed by applying the sensor-weighting matrix derived through the forward computation to the preprocessed signal vector, which yielded a time series corresponding to the location of interest. These virtual sensor data were then decomposed into time–frequency space per trial and averaged across the previously identified time–frequency extents (i.e., used in the beamformer analysis). This time–frequency analysis resulted in absolute amplitude estimates of each time–frequency domain response per participant for each condition and for every trial. These estimates were then used to compute a linear mixed-effects model of single-trial task performance (i.e., RT) on oscillatory neural dynamics (model =  $RT \sim \text{Condition} * \text{ResponseAmplitude}$ ; random effects =  $\sim 1 | \text{Participant/Trial}$ ) using the *nlme* toolbox in R. In addition, we computed the intertrial phase coherence (ITPC) from the extracted virtual sensors, which reflects the intertrial variability of the phase relationship at the single-trial level. These data were separately averaged over the alpha and theta spectral windows used in our beamformer analyses and the 350-ms time period prior to target onset and then compared between conditions.

## Results

### Behavioral Analysis

One participant was excluded from all analyses due to artifactual MEG data. The remaining 33 participants generally performed well on the task in both the spatially ( $M = 93.65\%$ ,  $SD = 5.42\%$ ) and temporally ( $M = 92.18\%$ ,  $SD = 6.17\%$ ) cued conditions. These differences in task performance and reaction time were statistically significant, such that participants were less accurate ( $t_{32} = 2.22$ ,  $P = 0.034$ ) and slower to respond ( $t_{32} = -5.73$ ,  $P < 0.001$ ) during temporally cued ( $M = 553.24$  ms,  $SD = 114.08$  ms) versus spatially cued ( $M = 527.03$  ms,  $SD = 103.79$  ms) trials. Importantly, the direction of these effects indicates that there was no speed-accuracy tradeoff in relation to the cueing effects on task performance. Behavioral metrics can be viewed in Figure 1B.

### MEG Sensor-Level Results

Time–frequency analysis of the sensor-level spectrograms across both conditions revealed 2 significant clusters of oscillatory responses to the task: one in the theta (3–6 Hz; 0–350 ms) and another in the alpha band (10–16 Hz; 250–500 ms; Fig. 2A), both of which were strongest in the gradiometers near posterior parietal and occipital cortices (both  $P$ 's  $< 0.001$ , corrected). Importantly, only time bins that ended no later than 500 ms after the cue onset were used in further analysis, as this

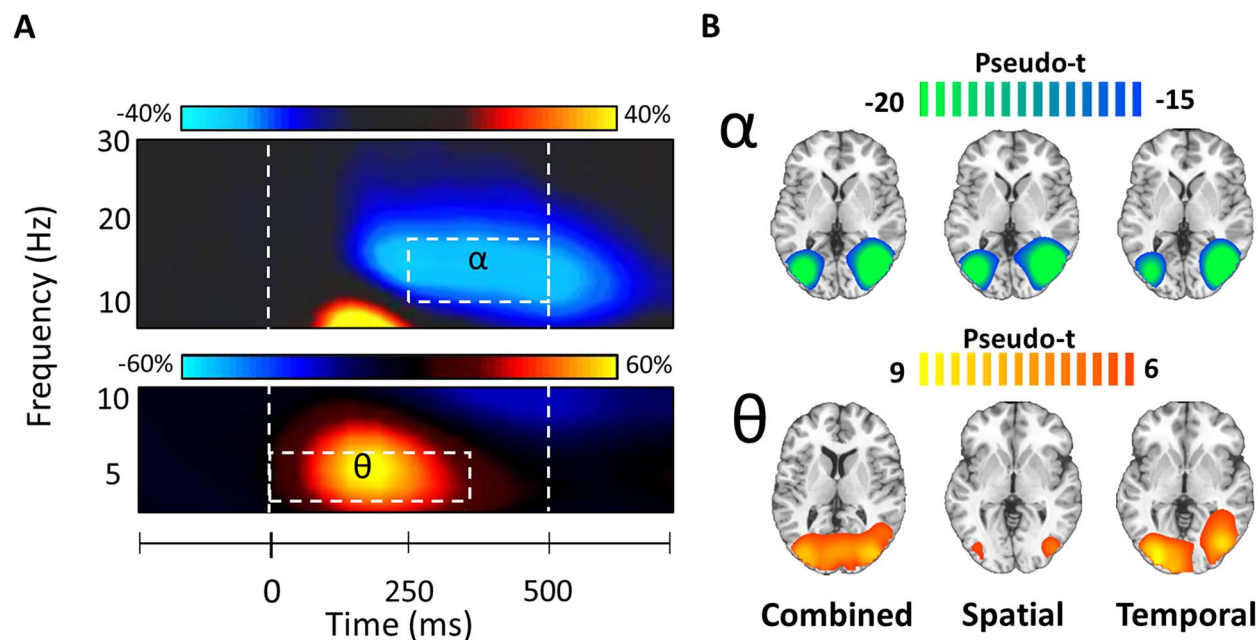


**Figure 2.** Grand averaged sensor-level time–frequency spectrograms and beamformer images for alpha and theta oscillatory responses. (A) Time–frequency spectrograms from representative sensors near occipitoparietal cortices showing oscillatory alpha (top; MEG2513 channel; 10–16 Hz; 250–500 ms;  $P < 0.001$ ) and theta (bottom; MEG2313; 3–6 Hz; 0–350 ms;  $P < 0.001$ ) responses averaged across trials and participants. Time is denoted on the x-axis and frequency is on the y-axis. The dotted line to the left (at 0 ms) indicates the onset of the attentional cue and the dotted line to the right (at 500 ms) represents the onset of the target stimulus for the shortest possible spatial cue duration (i.e.,  $900 \pm 400$  ms). Color bars above each spectrogram shows the percent change from baseline. (B) The desynchronization or decrease in alpha power was generated by neural populations in the bilateral occipital cortices, whereas synchronizations or increases in theta emerged from bilateral primary visual cortices. The color scale bar above each row of average maps indicates the response amplitude scale (in pseudo-t).

was the potential onset of the earliest target stimulus in the spatial cueing condition.

### MEG Source Results

To examine the neuroanatomical origins of the significant sensor-level oscillatory activity, each time–frequency bin was imaged using a frequency-resolved beamformer. The resulting images from each time–frequency response were first grand averaged per response across participants and conditions, which indicated that the increases in theta activity were strongest in the bilateral visual cortices, left precuneus, and superior parietal regions, whereas the strong decreases in alpha activity were distributed across bilateral lateral occipital cortices (Fig. 2B). The conditional averages are also available in Figure 2B.

We then computed whole-brain paired t-tests with cluster-based permutation correction to indicate which distinct neuroanatomical regions differ between the 2 cueing conditions. For the theta response, there was a significantly stronger increase following the temporal cue relative to the spatial cue in the left primary visual cortex (Fig. 3;  $P = 0.027$ , corrected). A significant cueing effect was also evident in the alpha band in left lateral occipital, right hippocampal, left posterior cingulate (PCC), and right dlPFC cortices (Fig. 4; all  $P$ 's  $< 0.001$ , corrected). In the left lateral occipital, right hippocampal, and posterior cingulate clusters the alpha decreases (from baseline) were stronger during the spatially cued trials relative to the temporally cued trials. In contrast, the right dlPFC exhibited essentially no alpha response during the spatially cued trials, along with an increase in alpha activity during temporally cued trials. Since gradiometers are primarily sensitive to cortical responses and less sensitive to deep brain signals, such as the hippocampus,

we repeated the alpha-band beamformer analysis using only the magnetometers in an attempt to validate our gradiometer findings. Consistent with the gradiometer findings, the magnetometer data indicated that the alpha oscillations (i.e., decreases from baseline) were stronger in the right hippocampus during spatially cued trials compared with temporally cued trials (Fig. 5;  $P < 0.001$ , corrected) thus supporting the veracity of our gradiometer findings.

### Relationships Between Single-Trial Neural Oscillatory Responses and Behavior

To investigate whether these neural dynamics were directly related to performance on our task, we extracted peak voxel virtual sensor time series from each of the clusters reported above, per each trial for every participant. We then conducted a time–frequency analysis of these data and averaged over the previously reported time–frequency bins (from the sensor analysis) for each oscillatory response and used the resulting values to compute single-trial linear mixed-effects models of task performance (i.e., RT) on neural response amplitude as a function of cueing condition. To account for the skewness of the MEG data, a log transform was applied. This analysis revealed a significant interaction between alpha responses in the right hippocampus and cueing condition on task performance, such that the positive relationship between hippocampal baseline alpha responses and reaction times (i.e., reduced absolute alpha activity predicted better task performance) was stronger in the spatially cued condition as compared with the temporally cued condition (Fig. 6;  $t_{2709} = -2.01$ ,  $P = 0.045$ ). Finally, we computed the ITPC to examine differences in phase consistency prior to target onset in each condition. These analyses indicated that

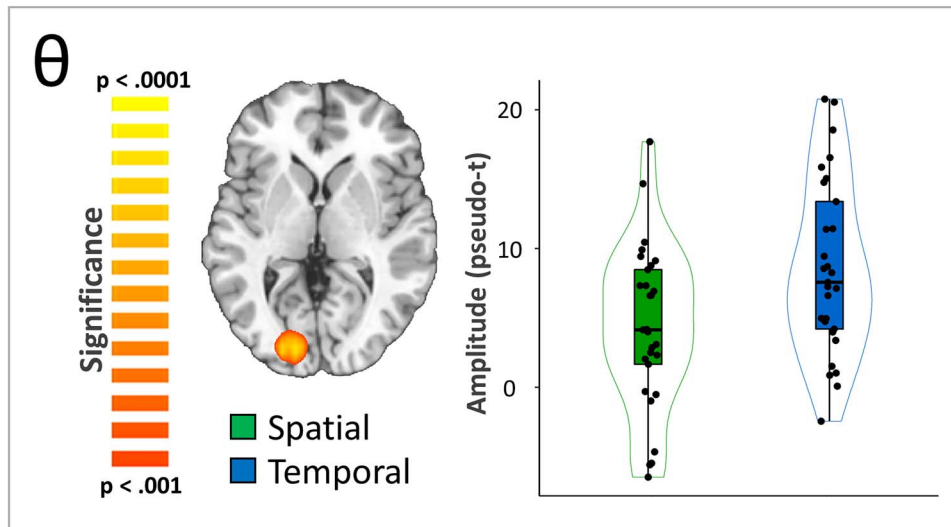


**Figure 3.** Effects of spatial versus temporal attentional orienting on theta activity. A whole-brain t-test revealed differences in theta response amplitude between conditions (i.e., temporal vs. spatial cueing). This effect was significant in the left occipital cortex (Talairach:  $-22, -88, 2$ ), where significantly stronger increases in theta activity in temporal relative to spatial trials was observed ( $P = 0.027$ , corrected).

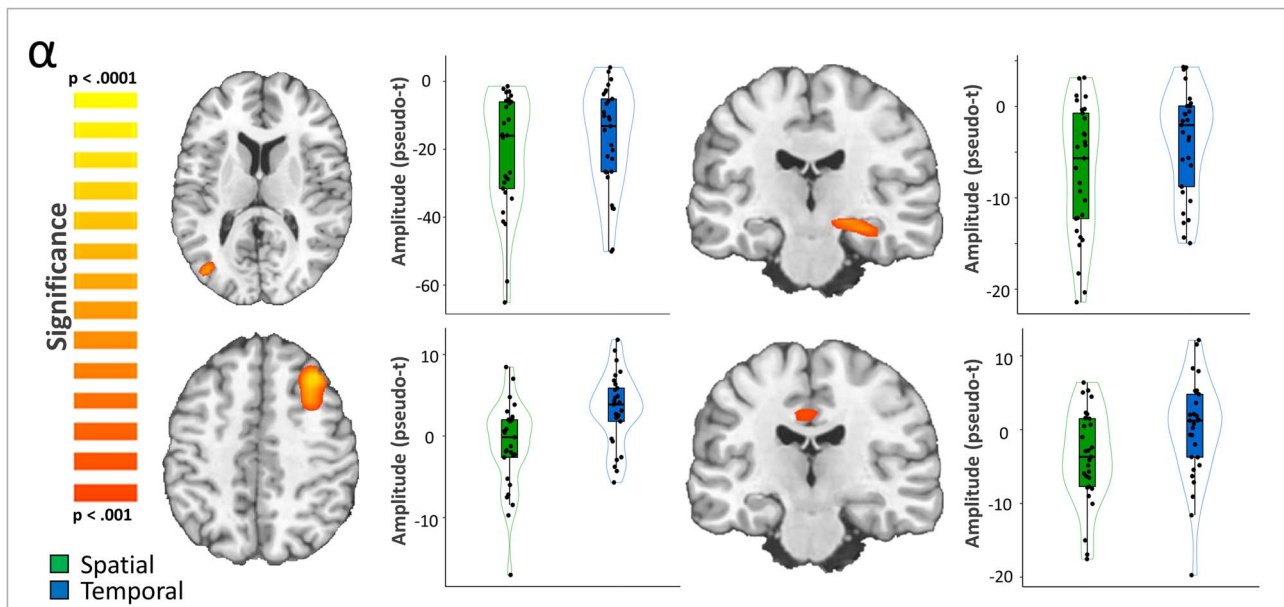


**Figure 4.** Effects of spatial versus temporal attentional orienting on alpha activity. A whole-brain t-test revealed differences in alpha response amplitude between conditions (i.e., temporal vs. spatial cueing). This effect was significant in the left lateral occipital cortex (top left; Talairach:  $-38, -73, 13$ ), right hippocampus (top right; Talairach:  $26, -20, -10$ ), and left PCC (bottom right; Talairach:  $-2, -25, 38$ ) with more robust decreases in alpha activity during spatially compared with temporally cued trials (all  $P$ 's  $< 0.001$ , corrected). In contrast, a significant cluster in the right dlPFC (bottom left; Talairach:  $30, 23, 41$ ) exhibited stronger increases in alpha during temporally cued in contrast to spatially cued trials ( $P < 0.001$ , corrected).

alpha ITPC did not differ between conditions (all  $P$ 's  $> 0.05$ ) but that the phase of theta oscillations was significantly more consistent (i.e., higher ITPC values) during temporal compared with spatial trials ( $P < 0.001$ ).

## Discussion

In this study, we used an adapted Posner (1980) task and MEG to identify the distinct neural oscillatory responses supporting attentional orienting to spatial and temporal cues. Foremost, our results indicated spectral specificity in the neural

responses underlying temporal and spatial attentional orienting across a set of regions commonly associated with visual attention. Specifically, stronger increases in theta (3–6 Hz) activity were observed during temporal orienting of attention within the primary visual cortex, whereas stronger decreases in alpha (10–16 Hz) were present in the lateral occipital, posterior cingulate, and hippocampal regions during the spatial orienting of attention. In contrast, an alpha increase was observed during temporal orienting in the right dlPFC, and this response was not seen during spatial orienting. Importantly, single-trial linear mixed-effects modeling revealed that the strength of the

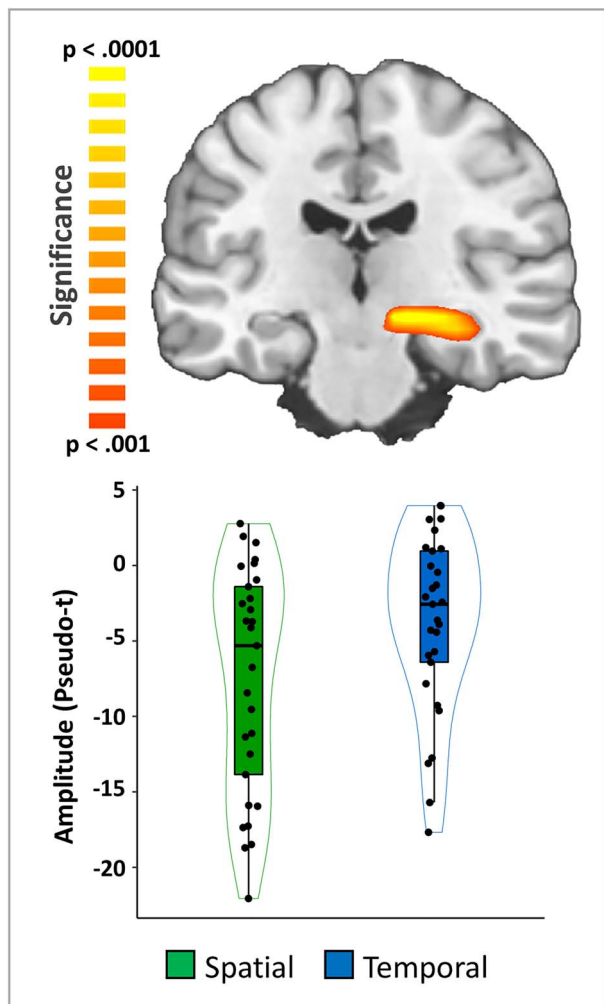


**Figure 5.** Validation of the alpha difference in the right hippocampus using magnetometers. A whole-brain voxel-wise t-test on the beamformer images computed using the magnetometers revealed a conditional difference in the right hippocampus that was very similar to that observed using the gradiometers (Fig. 4), with alpha decreases being much stronger in the spatial compared with the temporal cueing trials in the right hippocampus ( $P < 0.001$ , corrected).

alpha oscillatory response in the right hippocampus predicted improved performance more robustly during spatial compared with temporal orienting. Below we discuss the implications of these findings of spectral and spatial distinctions between the neural oscillations serving temporal and spatial orienting of attention.

We hypothesized that the underlying oscillatory dynamics involved in temporal and spatial attentional orienting would be spectrally specific, such that theta oscillations would be more engaged in temporal orienting and alpha oscillations being more essential to spatial orienting. In line with our hypothesis, stronger theta oscillations were observed during temporal compared with spatial orienting within the left primary visual cortex. This aligns well with previous literature, as theta oscillations are known to be critical in the visual system, principally for the temporal segmentation of information (Forte et al. 1999; Busch et al. 2009; Gupta et al. 2012; Landau and Fries 2012; Goodbourn and Forte 2013; Wiesman et al. 2017b). Moreover, the phase of the theta response prior to target onset was more consistent during

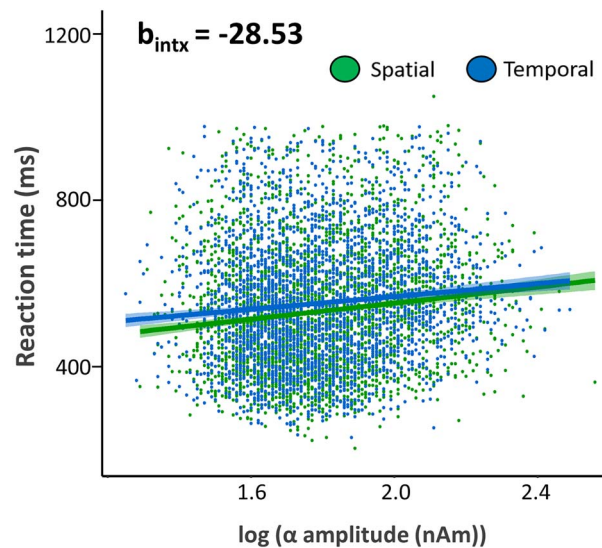


**Figure 6.** Impact of hippocampal neural activity on reaction time. A significant interaction between alpha responses in the right hippocampus and cueing condition was observed on reaction time, such that weaker absolute alpha activity in the spatially cued condition related more robustly to improved behavior (i.e., faster RT) relative to the temporally cued condition ( $t_{2709} = -2.01$ ,  $P = 0.045$ ). In addition, 95% confidence intervals are shown in blue and green for temporal and spatial conditions, respectively.

temporal trials relative to spatial trials in the left primary visual cortex, which may indicate the use of temporal information in the visual cortices during attentional allocation (Stefanics et al. 2010; Cravo et al. 2013). Thus, our findings extend this conceptualization and suggest that the temporal organization and segmentation of visual information is crucial for the temporal orienting of attention.

Also in agreement with our hypothesis, spatial orienting induced stronger alpha oscillations (i.e., decreases from baseline) relative to temporal orienting in the right hippocampus, left lateral occipital cortex, and left PCC. As mentioned previously, extant literature has demonstrated that alpha decreases (i.e., desynchronizations) in the posterior cortices during visual attention serves to disinhibit the processing of incoming visual information (Klimesch et al. 1998; Jensen and Mazaheri 2010; Dombrowe and Hilgetag 2014; van Diepen et al. 2016; Foster et al. 2017; McDermott et al. 2017; Wiesman et al. 2018, 2019; Wiesman and Wilson 2019, 2020b; McCusker et al. 2020). Thus, our finding of stronger alpha decreases during spatial versus temporal attentional orienting fits well with these widely reported results. In contrast, alpha frequency activity in the human hippocampus is less commonly reported; however, it has been shown to be important for the recollection of remembered spatial scenes (Herweg et al. 2016). Further, despite the relatively low sensitivity of MEG to deeper brain sources, we remain cautiously optimistic regarding this finding, as our task is particularly well designed to detect such signals. Specifically, the cueing portion of our task utilizes a relatively minor visual change and closely balances the visual stimulation present in each condition. This serves to reduce the amount of signal leakage from posterior occipital sources and likely allows us to measure other, less robust neural responses more accurately. Furthermore, our follow-up magnetometer analysis provided supportive evidence in regard to the veracity of this right hippocampal response. Hippocampal

response amplitude was also significantly related to task performance at the single-trial level, which further bolsters our confidence in this result. The right hippocampus is well established as being essential in associative learning and memory, particularly in visuospatial contexts (Witter and Amaral 1991; Moser et al. 1993, 2017; Burgess et al. 2002). Thus, we can speculate the hippocampus may exhibit preparatory alpha disinhibition during spatial attentional orienting; however, a more nuanced examination of the role of the right hippocampus in spatial orienting is certainly warranted in future studies.

A similar pattern of effects was also found in the left lateral occipital cortex, in which a more robust alpha decrease was observed during spatial orienting. Visual attention is typically thought to rely on cortical areas beyond the primary visual cortices during attention processing (Clark and Hillyard 1996; Tootell et al. 1998; Brefczynski and DeYoe 1999; Kanwisher and Wojciulik 2000). Therefore, this activity in the left lateral occipital cortex likely indicates better top-down control of functional information gating during spatial orienting. Such stronger alpha oscillatory activity during spatial orienting was also present in the PCC. Some studies suggest the PCC takes part in preparing neural attention resources during top-down visuospatial attention by connecting task motivation with attentional control (Small et al. 2003; Bagurdes et al. 2008). Within this framework, our finding of stronger responses during spatial relative to temporal orienting would suggest that the PCC assists in coordinating attentional control within the visual space.

In contrast to our other findings, there was a synchronization or increase in alpha activity during temporal orienting in the right dlPFC, and virtually no consistent alpha response was observed during spatial orienting. Previous neuroimaging literature supports the dlPFC as having an essential role in top-down spatial attentional processing and executive control (Knight et al. 1995; Daffner et al. 2000; Gehring and Knight 2002; Yamasaki et al. 2002; Rossi et al. 2009). As increases in alpha activity are often thought to reflect the inhibition incoming information or local processing (Sauseng et al. 2005; Händel et al. 2011; Wiesman and Wilson 2019), it is likely that the right dlPFC may have specifically been inhibited during temporal orienting, when spatial orienting would have been deleterious to performing the task at hand.

This study is not without limitations, with perhaps the most prominent being that the participants were all healthy young adults. To combat this limitation, future studies should utilize this task in different populations, such as a healthy aging population or patient populations who suffer from attentional deficits. Neuropsychological and neuroimaging research has found declines in attentional control and aberrations in the subsequent neural dynamics as a function of aging (Madden et al. 1997; Cabeza 2001; Kramer and Kray 2006; Persson et al. 2006; Madden 2007). Most recently, the oscillatory dynamics in reorienting attention have been found to be affected by the aging process in healthy adults (Arif et al. 2020), making this potential line of research all the more urgent. The absence of a “no cue” condition may also limit the findings of our study. Without a no cue condition, we could not fully confirm that the temporal cue had a significant orienting effect over no cue. However, if it were the case that the neural differences were explainable only by the spatial cue being more effective at orienting participants’ attention, we would expect that both the theta and the alpha responses would have been stronger (i.e., stronger theta synchronizations and alpha desynchronizations) in this condition, in line with previous literature (Sauseng et al. 2005;

Klimesch 2012; Landau and Fries 2012; van Diepen et al. 2016; Harris et al. 2017). However, our findings indicated that theta and alpha responses were systematically stronger for different types of attentional orienting, suggesting that these differing cue types were recruiting spatially and spectrally distinct neural resources. Nonetheless, future work using this task should consider adding a no cue condition, as this would strengthen the overall design and help confirm that different processes are fully engaged (Fan et al. 2002, 2005; Callejas et al. 2005). The relatively low task difficulty of this study is also a limiting factor. Altering the cognitive load of an attentional task has been shown to impact cueing effects during the orienting of attention (Santangelo et al. 2008), and thus, by varying load difficulty, future studies may provide more direct and perhaps discrete interpretations of our findings. Another existing limitation of this study lies in the relatively limited sensitivity of MEG to neural activity originating from subcortical areas. Though we observed an interesting and spectrally specific effect of attentional orienting in the hippocampus, other subcortical regions implicated in the orienting of attention may have been overlooked. Nascent methods in MEG, explicitly optically pumped magnetometers (OPM), have the potential to allow for more effective visualization of subcortical structures (Barry et al. 2019; Tierney et al. 2020). Thus, future studies with OPMS using this task could possibly address this limitation. A final potential future direction for this study, due to our spectrally specific findings within alpha and theta frequencies, would be to employ frequency-targeted neurostimulation in an attempt to causally dissociate attentional orienting networks. Supporting this, frequency-targeted neurostimulation (e.g., transcranial alternating current stimulation) has been demonstrated to influence oscillatory activity during visuospatial processing and top-down visual attention in a spectrally specific manner (Wiesman et al. 2018; Wilson et al. 2018; Clayton et al. 2019; McDermott et al. 2019; Spooner et al. 2020a).

To close, in this study we found that the distinct subtypes of attentional orienting are supported by discernible spectrally specific neural oscillations. Increases in theta activity appear to be more relevant for temporal orienting, particularly in visual areas. Conversely, decreases in alpha activity were stronger during spatial attentional orienting within regions associated with higher-order attentional networks. These findings are the first to empirically demonstrate the diverging oscillatory dynamics supporting the temporal and spatial orienting of attention and provide key knowledge for future studies of attentional processing, both in health and disease.

## Supplementary Material

Supplementary material can be found at *Cerebral Cortex* online.

## Funding

The National Institutes of Health (grants R01-MH116782 to T.W.W., R01-MH118013 to T.W.W., R01-DA047828 to T.W.W., RF1-MH117032 to T.W.W., F31-AG055332 to A.I.W., and F32-NS119375 to A.I.W.).

## Notes

We would like to thank the participants for volunteering to participate in the study as well as our staff and local collaborators for their contributions to the work. We would also like to

specifically thank Nichole Knott for extensive help with the MEG recordings. *Conflict of Interest*: None declared

## References

- Arif Y, Spooner RK, Wiesman AI, Embury CM, Proskovec AL, Wilson TW. 2020. Modulation of attention networks serving reorientation in healthy aging. *Aging*. 12:12582–12597.
- Atkinson MA, Simpson AA, Cole GG. 2018. Visual attention and action: how cueing, direct mapping, and social interactions drive orienting. *Psychon Bull Rev*. 25:1585–1605.
- Bagurdes LA, Mesulam MM, Gitelman DR, Weintraub S, Small DM. 2008. Modulation of the spatial attention network by incentives in healthy aging and mild cognitive impairment. *Neuropsychologia*. 46:2943–2948.
- Barry DN, Tierney TM, Holmes N, Boto E, Roberts G, Leggett J, Bowtell R, Brookes MJ, Barnes GR, Maguire EA. 2019. Imaging the human hippocampus with optically-pumped magnetoencephalography. *Neuroimage*. 203:116192.
- Brefczynski JA, DeYoe EA. 1999. A physiological correlate of the “spotlight” of visual attention. *Nat Neurosci*. 2:370–374.
- Burgess N, Maguire EA, O’Keefe J. 2002. The human hippocampus and spatial and episodic memory. *Neuron*. 35:625–641.
- Busch NA, Dubois J, VanRullen R. 2009. The phase of ongoing EEG oscillations predicts visual perception. *J Neurosci*. 29:7869–7876.
- Cabeza R. 2001. Cognitive neuroscience of aging: contributions of functional neuroimaging. *Scand J Psychol*. 42:277–286.
- Callejas A, Lupiáñez J, Funes MJ, Tudela P. 2005. Modulations among the alerting, orienting and executive control networks. *Exp Brain Res*. 167:27–37.
- Chang C-F, Hsu T-Y, Tseng P, Liang W-K, Tzeng OJL, Hung DL, Juan C-H. 2013. Right temporoparietal junction and attentional reorienting. *Hum Brain Mapp*. 34:869–877.
- Chun MM. 2000. Contextual cueing of visual attention. *Trends Cogn Sci*. 4:170–178.
- Chun MM, Jiang Y. 1998. Contextual cueing: implicit learning and memory of visual context guides spatial attention. *Cogn Psychol*. 36:28–71.
- Clark VP, Hillyard SA. 1996. Spatial selective attention affects early extrastriate but not striate components of the visual evoked potential. *J Cogn Neurosci*. 8:387–402.
- Clayton MS, Yeung N, Cohen KR. 2019. Electrical stimulation of alpha oscillations stabilizes performance on visual attention tasks. *J Exp Psychol Gen*. 148:203–220.
- Corbetta M, Shulman GL. 2002. Control of goal-directed and stimulus-driven attention in the brain. *Nat Rev Neurosci*. 3:201–215.
- Coull JT, Frith CD, Büchel C, Nobre AC. 2000. Orienting attention in time: behavioural and neuroanatomical distinction between exogenous and endogenous shifts. *Neuropsychologia*. 38:808–819.
- Coull JT, Nobre AC. 1998. Where and when to pay attention: the neural systems for directing attention to spatial locations and to time intervals as revealed by both PET and fMRI. *J Neurosci*. 18:7426–7435.
- Cravo AM, Rohenkohl G, Wyart V, Nobre AC. 2013. Temporal expectation enhances contrast sensitivity by phase entrainment of low-frequency oscillations in visual cortex. *J Neurosci*. 33:4002–4010.
- Daffner KR, Mesulam MM, Scinto LFM, Acar D, Calvo V, Faust R, Chabrierie A, Kennedy B, Holcomb P. 2000. The central role of the prefrontal cortex in directing attention to novel events. *Brain*. 123:927–939.
- Doesburg SM, Bedo N, Ward LM. 2016. Top-down alpha oscillatory network interactions during visuospatial attention orienting. *Neuroimage*. 132:512–519.
- Dombrowe I, Hilgetag CC. 2014. Occipitoparietal alpha-band responses to the graded allocation of top-down spatial attention. *J Neurophysiol*. 112:1307–1316.
- Ernst MD. 2004. Permutation methods: a basis for exact inference. *Stat Sci*. 19:676–685.
- Fan J, McCandliss BD, Fossella J, Flombaum JI, Posner MI. 2005. The activation of attentional networks. *Neuroimage*. 26:471–479.
- Fan J, McCandliss BD, Sommer T, Raz A, Posner MI. 2002. Testing the efficiency and independence of attentional networks. *J Cogn Neurosci*. 14:340–347.
- Forte J, Hogben JH, Ross J. 1999. Spatial limitations of temporal segmentation. *Vision Res*. 39:4052–4061.
- Foster JJ, Sutterer DW, Serences JT, Vogel EK, Awh E. 2017. Alpha-band oscillations enable spatially and temporally resolved tracking of covert spatial attention. *Psychol Sci*. 28:929–941.
- Gehring WJ, Knight RT. 2002. Lateral prefrontal damage affects processing selection but not attention switching. *Cogn Brain Res*. 13:267–279.
- Goodbourn PT, Forte JD. 2013. Spatial limitations of fast temporal segmentation are best modeled by V1 receptive fields. *J Vis*. 13:23–23.
- Gross J, Kujala J, Hämäläinen M, Timmermann L, Schnitzler A, Salmelin R. 2001. Dynamic imaging of coherent sources: studying neural interactions in the human brain. *Proc Natl Acad Sci*. 98:694–699.
- Gupta AS, van der Meer MAA, Touretzky DS, Redish AD. 2012. Segmentation of spatial experience by hippocampal theta sequences. *Nat Neurosci*. 15:1032–1039.
- Händel BF, Haarmeier T, Jensen O. 2011. Alpha oscillations correlate with the successful inhibition of unattended stimuli. *J Cogn Neurosci*. 23:2494–2502.
- Harris AM, Dux PE, Jones CN, Mattingley JB. 2017. Distinct roles of theta and alpha oscillations in the involuntary capture of goal-directed attention. *Neuroimage*. 152:171–183.
- Herweg NA, Apitz T, Leicht G, Fuentemilla L, Bunzeck N. 2016. Theta-alpha oscillations bind the hippocampus, prefrontal cortex, and striatum during recollection: evidence from simultaneous EEG–fMRI. *J Neurosci*. 36:3579–3587.
- Higuchi Y, Ueda Y, Ogawa H, Saiki J. 2016. Task-relevant information is prioritized in spatiotemporal contextual cueing. *Atten Percept Psychophys*. 78:2397–2410.
- Hillebrand A, Singh KD, Holliday IE, Furlong PL, Barnes GR. 2005. A new approach to neuroimaging with magnetoencephalography. *Hum Brain Mapp*. 25:199–211.
- Jensen O. 2006. Maintenance of multiple working memory items by temporal segmentation. *Neuroscience*. 139:237–249.
- Jensen O, Mazaheri A. 2010. Shaping functional architecture by oscillatory alpha activity: gating by inhibition. *Front Hum Neurosci*. 4. doi: 10.3389/fnhum.2010.00186.
- Jiang YV, Sisk CA. 2020. Contextual cueing. In: Pollmann S, editor. *Spatial learning and attention guidance*. *Neuromethods*. New York: Springer, pp. 59–72.
- Kanwisher N, Wojciulik E. 2000. Visual attention: insights from brain imaging. *Nat Rev Neurosci*. 1:91–100.
- Klimesch W. 2012. Alpha-band oscillations, attention, and controlled access to stored information. *Trends Cogn Sci*. 16:606–617.

- Klimesch W, Doppelmayr M, Russegger H, Pachinger T, Schwaiger J. 1998. Induced alpha band power changes in the human EEG and attention. *Neurosci Lett.* 244:73–76.
- Knight RT, Grabowecy MF, Scabini D. 1995. Role of human prefrontal cortex in attention control. *Adv Neurol.* 66:21–34 discussion 34–36.
- Kovach CK, Gander PE. 2016. The demodulated band transform. *J Neurosci Methods.* 261:135–154.
- Kramer AF, Kray J. 2006. Aging and Attention. In: *Lifespan cognition: mechanisms of change.* New York: Oxford University Press, pp. 57–69.
- Kurz MJ, Wiesman AI, Coolidge NM, Wilson TW. 2018. Children with cerebral palsy hyper-gate somatosensory stimulations of the foot. *Cereb Cortex.* 28:2431–2438.
- Landau AN, Fries P. 2012. Attention samples stimuli rhythmically. *Curr Biol.* 22:1000–1004.
- Madden DJ. 2007. Aging and visual attention. *Curr Dir Psychol Sci.* 16:70–74.
- Madden DJ, Turkington TG, Provenzale JM, Hawk TC, Hoffman JM, Coleman RE. 1997. Selective and divided visual attention: age-related changes in regional cerebral blood flow measured by H215O PET. *Hum Brain Mapp.* 5:389–409.
- Maris E, Oostenveld R. 2007. Nonparametric statistical testing of EEG- and MEG-data. *J Neurosci Methods.* 164:177–190.
- McCusker MC, Wiesman AI, Schantell MD, Eastman JA, Wilson TW. 2020. Multi-spectral oscillatory dynamics serving directed and divided attention. *Neuroimage.* 217:116927.
- McDermott TJ, Wiesman AI, Mills MS, Spooner RK, Coolidge NM, Proskovec AL, Heinrichs-Graham E, Wilson TW. 2019. tDCS modulates behavioral performance and the neural oscillatory dynamics serving visual selective attention. *Hum Brain Mapp.* 40:729–740.
- McDermott TJ, Wiesman AI, Proskovec AL, Heinrichs-Graham E, Wilson TW. 2017. Spatiotemporal oscillatory dynamics of visual selective attention during a flanker task. *Neuroimage.* 156:277–285.
- Moser E, Moser M, Andersen P. 1993. Spatial learning impairment parallels the magnitude of dorsal hippocampal lesions, but is hardly present following ventral lesions. *J Neurosci.* 13:3916–3925.
- Moser EI, Moser M-B, McNaughton BL. 2017. Spatial representation in the hippocampal formation: a history. *Nat Neurosci.* 20:1448–1464.
- Nagata Y, Bayless SJ, Mills T, Taylor MJ. 2012. Spatio-temporal localisation of attentional orienting to gaze and peripheral cues. *Brain Res.* 1439:44–53.
- Olson IR, Chun MM. 2001. Temporal contextual cuing of visual attention. *J Exp Psychol Learn Mem Cogn.* 27:1299–1313.
- Papp N, Ktonas P. 1977. Critical evaluation of complex demodulation techniques for the quantification of bioelectrical activity. *Biomed Sci Instrum.* 13:135–145.
- Persson J, Nyberg L, Lind J, Larsson A, Nilsson L-G, Ingvar M, Buckner RL. 2006. Structure–function correlates of cognitive decline in aging. *Cereb Cortex.* 16:907–915.
- Posner MI. 1980. Orienting of attention. *Q J Exp Psychol.* 32:3–25.
- Proskovec AL, Heinrichs-Graham E, Wiesman AI, McDermott TJ, Wilson TW. 2018. Oscillatory dynamics in the dorsal and ventral attention networks during the reorienting of attention. *Hum Brain Mapp.* 39:2177–2190.
- Roberts BM, Hsieh L-T, Ranganath C. 2013. Oscillatory activity during maintenance of spatial and temporal information in working memory. *Neuropsychologia.* 51:349–357.
- Rossi AF, Pessoa L, Desimone R, Ungerleider LG. 2009. The prefrontal cortex and the executive control of attention. *Exp Brain Res.* 192:489–497.
- Santangelo V, Finoia P, Raffone A, Olivetti Belardinelli M, Spence C. 2008. Perceptual load affects exogenous spatial orienting while working memory load does not. *Exp Brain Res.* 184:371–382.
- Sauseng P, Klimesch W, Doppelmayr M, Pecherstorfer T, Freunberger R, Hanslmayr S. 2005. EEG alpha synchronization and functional coupling during top-down processing in a working memory task. *Hum Brain Mapp.* 26:148–155.
- Small DM, Gitelman DR, Gregory MD, Nobre AC, Parrish TB, Mesulam M-M. 2003. The posterior cingulate and medial prefrontal cortex mediate the anticipatory allocation of spatial attention. *Neuroimage.* 18:633–641.
- Snyder JJ, Chatterjee A. 2006. The frontal cortex and exogenous attentional orienting. *J Cogn Neurosci.* 18:1913–1923.
- Spooner RK, Eastman JA, Rezich MT, Wilson TW. 2020a. High-definition transcranial direct current stimulation dissociates fronto-visual theta lateralization during visual selective attention. *J Physiol.* 598:987–998.
- Spooner RK, Wiesman AI, Mills MS, O’Neill J, Robertson KR, Fox HS, Swindells S, Wilson TW. 2018. Aberrant oscillatory dynamics during somatosensory processing in HIV-infected adults. *NeuroImage Clin.* 20:85–91.
- Spooner RK, Wiesman AI, Proskovec AL, Heinrichs-Graham E, Wilson TW. 2019. Rhythmic spontaneous activity mediates the age-related decline in somatosensory function. *Cereb Cortex.* 29:680–688.
- Spooner RK, Wiesman AI, Proskovec AL, Heinrichs-Graham E, Wilson TW. 2020b. Prefrontal theta modulates sensorimotor gamma networks during the reorienting of attention. *Hum Brain Mapp.* 41:520–529.
- Stefanics G, Hangya B, Hernádi I, Winkler I, Lakatos P, Ulbert I. 2010. Phase entrainment of human delta oscillations can mediate the effects of expectation on reaction speed. *J Neurosci.* 30:13578–13585.
- Taulu S, Simola J. 2006. Spatiotemporal signal space separation method for rejecting nearby interference in MEG measurements. *Phys Med Biol.* 51:1759–1768.
- Tierney TM, Levy A, Barry DN, Meyer SS, Shigihara Y, Everatt M, Mellor S, Lopez JD, Bestmann S, Holmes N, et al. 2020. Mouth magnetoencephalography: a unique perspective on the human hippocampus. *bioRxiv.* 2020.03.19.998641.
- Tootell RBH, Hadjikhani N, Hall EK, Marrett S, Vanduffel W, Vaughan JT, Dale AM. 1998. The retinotopy of visual spatial attention. *Neuron.* 21:1409–1422.
- Uusitalo MA, Ilmoniemi RJ. 1997. Signal-space projection method for separating MEG or EEG into components. *Med Biol Eng Comput.* 35:135–140.
- van Diepen RM, Miller LM, Mazaheri A, Geng JJ. 2016. The role of alpha activity in spatial and feature-based attention. *eNeuro.* 3:1–11.
- Van Veen BD, Van Drongelen W, Yuchtman M, Suzuki A. 1997. Localization of brain electrical activity via linearly constrained minimum variance spatial filtering. *IEEE Trans Biomed Eng.* 44:867–880.
- Wiesman AI, Groff BR, Wilson TW. 2019. Frontoparietal networks mediate the behavioral impact of alpha inhibition in visual cortex. *Cereb Cortex.* 29:3505–3513.
- Wiesman AI, Heinrichs-Graham E, Coolidge NM, Gehringer JE, Kurz MJ, Wilson TW. 2017a. Oscillatory dynamics and

- functional connectivity during gating of primary somatosensory responses. *J Physiol*. 595:1365–1375.
- Wiesman AI, Heinrichs-Graham E, Proskovec AL, McDermott TJ, Wilson TW. 2017b. Oscillations during observations: dynamic oscillatory networks serving visuospatial attention. *Hum Brain Mapp*. 38:5128–5140.
- Wiesman AI, Mills MS, McDermott TJ, Spooner RK, Coolidge NM, Wilson TW. 2018. Polarity-dependent modulation of multi-spectral neuronal activity by transcranial direct current stimulation. *Cortex*. 108:222–233.
- Wiesman AI, Wilson TW. 2019. Alpha frequency entrainment reduces the effect of visual distractors. *J Cogn Neurosci*. 31:1392–1403.
- Wiesman AI, Wilson TW. 2020a. Attention modulates the gating of primary somatosensory oscillations. *Neuroimage*. 211:116610.
- Wiesman AI, Wilson TW. 2020b. Posterior alpha and gamma oscillations index divergent and superadditive effects of cognitive interference. *Cereb Cortex*. 30:1931–1945.
- Wilson TW, Heinrichs-Graham E, Proskovec AL, McDermott TJ. 2016. Neuroimaging with magnetoencephalography: A dynamic view of brain pathophysiology. *Transl Res*. 175: 17–36.
- Wilson TW, McDermott TJ, Mills MS, Coolidge NM, Heinrichs-Graham E. 2018. tDCS modulates visual gamma oscillations and basal alpha activity in occipital cortices: evidence from MEG. *Cereb Cortex N Y N*. 28: 1597–1609.
- Witter MP, Amaral DG. 1991. Entorhinal cortex of the monkey: V. projections to the dentate gyrus, hippocampus, and subicular complex. *J Comp Neurol*. 307:437–459.
- Yamasaki H, LaBar KS, McCarthy G. 2002. Dissociable prefrontal brain systems for attention and emotion. *Proc Natl Acad Sci*. 99:11447–11451.
- Yantis S. 2002. Stimulus-driven and goal-directed attentional control. In: Cantoni V, Marinaro M, Petrosino A, editors. *Visual attention mechanisms*. Boston: Springer, pp. 125–134.